Investigating the best topology for Traction Power Substations (TPSs) in a Medium Voltage DC (MVDC) railway electrification system

Sharifi, Sina; Kamel, Tamer; Tricoli, Pietro

Investigating the best topology for Traction Power Substations (TPSs) in a Medium Voltage DC (MVDC) railway electrification system

Sina Sharifi, Tamer Kamel, and Pietro Tricoli, member, IEEE
Birmingham Centre for Railway Research and Education (BCRRE), University of Birmingham Edgbaston,
Birmingham, United Kingdom
E-Mail: sina.sharifi.90@gmail.com

Acknowledgements

"This project has received funding from the Shift2Rail Joint Undertaking (JU) under grant agreement No 826238. The JU receives support from the European Union's Horizon 2020 research and innovation programme and the Shift2Rail JU members other than the Union".

Keywords

«AC-DC converter», «Medium voltage converter», «DC railway power supply», «Design», «Analytical losses computation».

Abstract

Medium or high voltage DC railway electrification systems have been proposed since 1989. Such systems benefit from lowest conduction losses and voltage drops typical of DC systems and can efficiently integrate renewable energy sources in the railway supply system. However, no industrial application has been developed for the limitations connected to DC switchgears and voltage transformation on the trains. The first limitation can be addressed with a suitable power converter topology for medium voltage DC (MVDC) traction power substations (TPSs) with a controlled output current. In this paper, three different AC-DC converter topologies, i.e., bi-directional thyristor converter, cascaded two-level voltage source converter (VSC), and modular multilevel converter with full-bridge submodules (MMC-FB), are analytically compared in terms of their efficiencies and device requirements for application to MVDC TPSs.

Introduction

Currently, AC electrification at medium voltage level is used for mainline and high-speed railways to reduce the transmission losses and the voltage drop. Because of the single-phase supply, the TPSs cause imbalance on the public grid and, as such, they need to be connected to a high-voltage transmission line, that usually involve expensive equipment and connection works. Moreover, high-voltage transmission lines are not always close to the TPSs, further increasing the connection costs. On the other hand, MVDC electrification systems would not cause imbalance on the grid because they can use 3-phase ac/dc converters. This means they can potentially be connected to distribution grids, thereby reducing the installation costs. Other advantages of DC supply systems over AC supply systems are the lower voltage drops, as the inductance does not cause any effect, and the lack of skin effect that reduce the resistance of the line. Also, all the sections of the electrified line can be connected together, as there is no risk of power circulation in parallel to the grid, and so neutral sections are not required. In addition, DC electrification systems would be the suitable choice for integrating renewable power sources in the railway electrification system, which has recently attracted much attention from scientists [1].

AC- DC converters are the key components in MVDC TPSs and selecting the most appropriate is a crucial task. In [2] and [3], a modular multilevel converter (MMC) with half-bridge submodules has been proposed for AC-DC conversion in MVDC railways. The authors of [4] have suggested 12-pulse diode rectifiers, which should be protected by solid state DC circuit breakers. The authors of [5] and [6] have introduced series connected 24-pulse diode converters as the most efficient topology for MVDC TPSs, albeit with an unregulated DC output. In [7] and [8], a thyristor rectifier has been chosen for TPSs to regulate the DC output voltage and limit the short-circuit current. Series

connection of converter cells in both AC and DC sides has been introduced in [9], where each converter cell consists of a VSC connected to a cycloconverter via a medium frequency transformer. However, there is no comprehensive study which introduces operational specifications of MVDC TPSs and compares various AC-DC converter topologies in detail. This paper presents the specifications of a MVDC railway electrification system and investigates three different converter's topologies for its TPSs. The selected topologies are a bi-directional thyristor converter, a cascaded two-level VSC, and MMC with full-bridge submodules. The number of required series and parallel power electronic switches is determined, and the power efficiency of these converters is analytically studied to compare the three topologies.

MVDC RAILWAY ELECTRIFICATION SYSTEM SPECIFICATIONS

In order to use some of the existing 25 kV AC infrastructure, the nominal voltage for the MVDC supply system has been chosen at 25 kV DC. Therefore, the MVDC railway supply system can use standards similar to those of 25 kV AC railway [10] to define its operational conditions, as shown in Table I.

The MVDC supply system is designed to supply mainline and high-speed lines. Considering at least two AC-DC converters in each MVDC TPS, the specifications of converters are summarised in Table II. The converter is connected to the medium voltage AC distribution grid and can inject the regenerated braking energy from the trains into the grid. The nominal DC side voltage of the converter is chosen to be equal to the no-load voltage of the system, ensuring suitable voltage regulation at the converter bus bars.

As the worst case, and based on typical values for conventional DC supply system [11], it is considered that the converter must deliver 450% of nominal DC current for a maximum of 10 seconds. As the semiconductor devices have only a very limited overloading capacity, it is necessary to design the converter for the worst case, thus adding several semiconductor devices in parallel.

Table I: Operational conditions of the MVDC railway electrification system

Lowest non-permanent voltage	U_{min2}	17.5 kV	Highest permanent voltage	U_{max1}	27.5 kV
Lowest permanent voltage	U_{min1}	19 kV	Highest non-permanent voltage	U_{max2}	29 kV
Nominal voltage	$V_{sys,nom}$	25 kV	Maximum voltage during long-term overvoltages	U_{max3}	38.75 kV

Table II: Specifications of AC-DC converters in the MVDC TPS

Power rating	$P_{converter}$	30 MW
Nominal DC voltage	$V_{DC,nom}$	27.5 kV
Maximum DC voltage in overvoltage condition	$V_{DC,overvoltage}$	38.75 kV
Nominal DC current	$I_{DC,nom}$	1.09 kA
Maximum DC current in overload condition	$I_{DC,overload}$	4.91 kA

METHODOLOGY

A) Bi-directional thyristor converter

The thyristor rectifier is widely used in High-Voltage DC (HVDC) power substations. Moreover, 12-pulse thyristor rectifier has been implemented for low voltage DC railway electrification systems [12]. In order to inject the regenerative braking energy, an anti-parallel 12-pulse thyristor inverter is connected to the rectifier, as shown in Fig. 1 (a). In this section, specifications and losses of a 6-pulse rectifier are calculated first. Then, the calculations are extended to the 12-pulse rectifier and inverter. Fig. 2 depicts output voltage-current characteristics of the 6-pulse thyristor rectifier. Fig. 1 (b) shows the single-phase model of the transformer, where $\bar{\boldsymbol{V}}_s$, $\bar{\boldsymbol{V}}_{AC}$ and $\bar{\boldsymbol{I}}_{AC,1}$ are the phasor forms of the phase voltage at the transformer's secondary, input phase voltage of the 6-pulse rectifier, and the fundamental component of the phase current, respectively. $\bar{\boldsymbol{V}}_s$ and $\bar{\boldsymbol{I}}_{AC,1}$ are assumed to be in phase.

Under normal operation conditions, the average output voltage and the peak value of the phase current are calculated as follows [13]:

$$V_{DC,avg} = \frac{3\sqrt{3}}{\pi} V_{AC,peak} \cos\alpha - \frac{3}{\pi}\omega L_s I_{DC} \quad , \quad I_{AC,peak,1} \cong \frac{2\sqrt{3}}{\pi} I_{DC} \tag{1}$$

where α is the thyristors' firing angle, ω is the angular frequency of the AC supply (100 rad/s) and L_s is the transformer inductance in each phase. The KVL in the transformer model yields to:

$$\bar{\boldsymbol{V}}_{AC} = \bar{\boldsymbol{V}}_s - j\omega L_s \bar{\boldsymbol{I}}_{AC,1} \tag{2}$$

According to Fig. 2, at the point O, the DC current $I_{DC,O}$ equals to 150% of $I_{DC,nom}$. Using (1) and (2):

$$V_{DC,avg,O} = \frac{3\sqrt{3}}{\pi}\left|\bar{\boldsymbol{V}}_s - j\omega L_s \bar{\boldsymbol{I}}_{AC,1,O}\right| - \frac{3}{\pi}\omega L_s I_{DC,O} \tag{3}$$

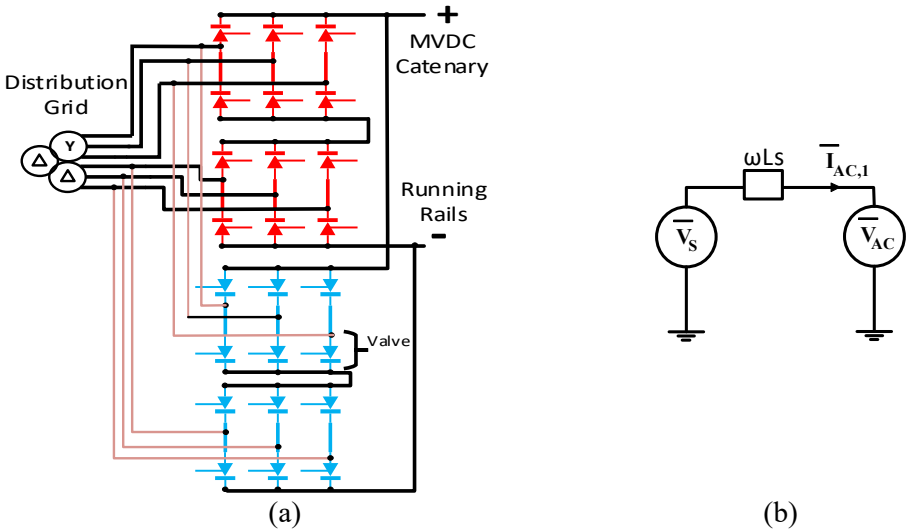

Fig. 1: (a) 12-pulse thyristor rectifier and inverter in anti-parallel configuration (b) Single phase model of TPS transformer

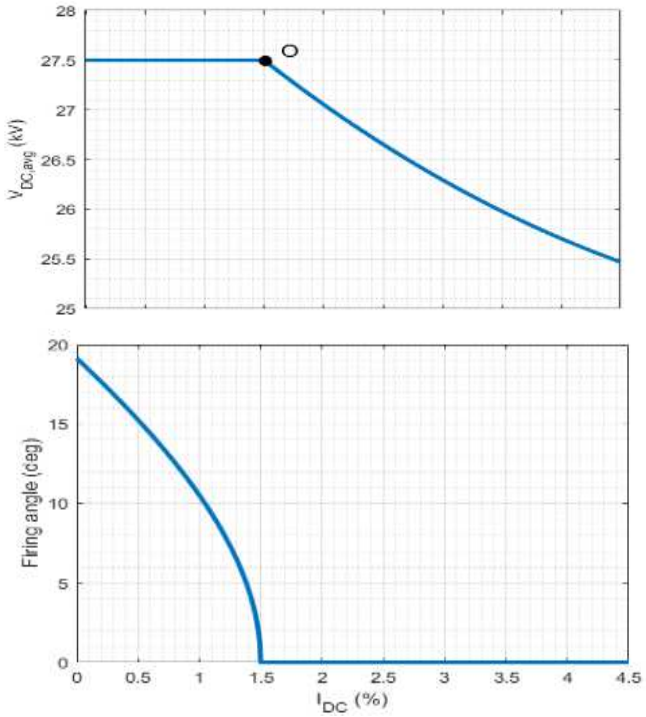

Fig. 2: The 6-pulse thyristor rectifier: Average DC voltage and firing angle versus DC current

The apparent power of the transformer is chosen as 40 MVA and a typical value for its reactance is 0.01 pu. Therefore:

$$\omega L_s = X = \frac{V_{s,rms,L-L}{}^2}{S_{base}} X_{pu} = \frac{3\,V_s{}^2}{2\,S_{base}} X_{pu} = \frac{0.03\,V_s{}^2}{80 \times 10^6} \quad (4)$$

where $V_{s,rms,L-L}$ is nominal line-to-line voltage of secondary side and S_{base} is base value for apparent power of the transformer. Substituting (4) and $I_{AC,peak,1}$ from (1) into (3) leads to a quartic equation of V_s, which has only one feasible solution, i.e., $\overline{\boldsymbol{V}}_s = 17.60\ kV \angle 0°$ (17.6 kV is the peak value of $\overline{\boldsymbol{V}}_s$).

The thyristor ABB 5STP 18M6500 [14] is chosen for implementing the thyristor converter. The maximum surge peak forward ($V_{DSM,thy}$) for this thyristor is 6.5 kV. The converter must operate in the overvoltage condition, where the DC side voltage may reach to U_{max3}. Based on operating principal of the converter [13], the highest voltage that a thyristor valve must block equals to the peak value of the line-to-line voltage. Using (1) and assuming zero firing angle and maximum power of 30 MW at overvoltage condition (i.e., maximum DC current of 0.77 kA), the voltage $V_{AC,L-L,peak,overvoltage}$ equals to 41.49 kV. With uniform voltage sharing between series thyristors in each valve, the number of required series thyristors is calculated as follows [15]:

$$V_{DSM}\ or\ V_{RSM} = k \times V_{AC,L-L,peak,overvoltage} = 2.5 * 41.49\,\text{kV} = 103.70\,\text{kV} \quad (5)$$

$$N_s = ceil\left(\frac{V_{DSM}}{V_{DSM,thy}}\right) = 16 \quad (6)$$

where N_s is the number of required series thyristors in each valve of the 6-pulse rectifier, V_{DSM} and V_{RSM} are maximum surge peak forward and reverse blocking voltage applied to each valve, and k is a safety factor related to quality of the AC network, in terms of overvoltage transients. For industrial environments, k is normally selected between 2 and 2.5.

The maximum current of each thyristor valve equals to the DC current in overload condition ($I_{DC,overload}$). Considering the DC current shape to be rectangular, the average and RMS current of each thyristor valve in the worst case are evaluated as follows:

$$(I_{valve,avg})_{max} = \frac{I_{DC,overload}}{3} = 1.64\ kA,$$
$$(I_{valve,rms})_{max} = \frac{I_{DC,overload}}{\sqrt{3}} = 2.83\ kA \quad (7)$$

The selected thyristor can handle the average and RMS current ($I_{T(AV)M}$ and $I_{T(RMS)}$) of 1.8 kA and 2.82 kA, respectively. In addition, $I_{T(AV)M}$ has been measured by a half-sine wave in the datasheet, which means the peak of the half-sine wave equals to 5.65 kA. This value is greater than $I_{DC,overload}$. Hence, one thyristor is sufficient to deliver the overload current and the number of required parallel thyristors in each valve (N_p) equals to one.

In this paper, the losses related to the transformer, thyristors' gate circuits, and blocking mode of thyristors are neglected. The switching and conduction losses of each thyristor are calculated as follows [16]:

$$P_{conduction\ losses,thyristor} = V_{(T0)}\,I_{T,avg} + r_T\,I_{T,rms}{}^2 \quad (8)$$

$$P_{switching\ losses,thyristor} = f\,(W_{off} + W_{on}) \quad (9)$$

$$P_{total\ losses,rectifier} = 6 \times N_s \times N_p \times P_{losses,thyristor} \quad (10)$$

where $V_{(T0)}$ is threshold voltage, $I_{T,avg}$ and $I_{T,rms}$ are average and RMS current of valve, r_T is slope resistance, f is AC supply frequency (50 Hz), and W_{off} and W_{on} are thyristor turn-off and turn-on energy losses. The thyristor's datasheet provides curves for W_{off} and W_{on}. In determining W_{off}, the parameter V_0 is peak of the line-to-line AC voltage in nominal operation [17] divided by the number of series thyristors, which can be calculated using (2) and $I_{AC,peak,1}$ from (1). For calculating W_{on}, the maximum forward current of the thyristor (I_{TRM}) is assumed to be equal to the DC side current.

In the 12-pulse rectifier which is designed for the MVDC railway, there are two series connected 6-pulse rectifiers with nominal DC voltage of $\frac{V_{DC,nom}}{2}$. The nominal output current for each 6-pulse rectifier is the same as previous case ($I_{DC,nom}$). All the formulas for 6-pulse rectifier are assumed to be valid for the 12-pulse rectifier.

To have the same voltage drop in the transformer model in comparison to the 27.5 kV 6-pulse rectifier, ωL_s for star and delta connection are assumed to be two times of the previous case (because each 6-pulse rectifiers supply half of the AC current). The number of series connected thyristors in one valve of 12-pulse rectifier is therefore 9. Similar to 6-pulse rectifier, one thyristor is sufficient to carry

the valve current. In calculating V_0 for each 6-pulse rectifier, the peak of the line-to-line AC voltage is supposed to be equal to half of the value for 27.5 kV 6-pulse rectifier.

12-pulse rectifier and 12-pulse inverter in anti-parallel configuration

As the regenerative power is smaller than the train's consumption, the current rating for the inverter is approximately 30% of that of the rectifier, so a value of 50% has been chosen for the calculations. The 12-pulse inverter consists of two series connected 6-pulse inverters, with nominal voltage of $\frac{V_{DC,nom}}{2}$ and nominal current of $\frac{I_{DC,nom}}{2}$.

Since the inverter and the rectifier are connected in parallel, the voltage that each thyristor valve in the inverter must block is the same as the rectifier. Therefore, the number of series thyristors in each valve is the same as the 12-pulse rectifier. The number of required parallel thyristors is one. The inverter loss analysis is done similar to the 12-pulse rectifier.

Fig. 3 (a) shows the power efficiency of the 12-pulse rectifier and inverter for different DC currents. In the interval between 30% to 450% of the nominal DC current, the efficiency is above 99%. Fig. 3 (b) depicts the switching and conduction losses of 12-pulse rectifier for various DC loads. The switching losses are below 100 kW and increase slightly with the load current. However, they are the dominant type of losses between 10% and 110% of the load, indicating the importance of evaluating switching losses in medium voltage thyristor converters.

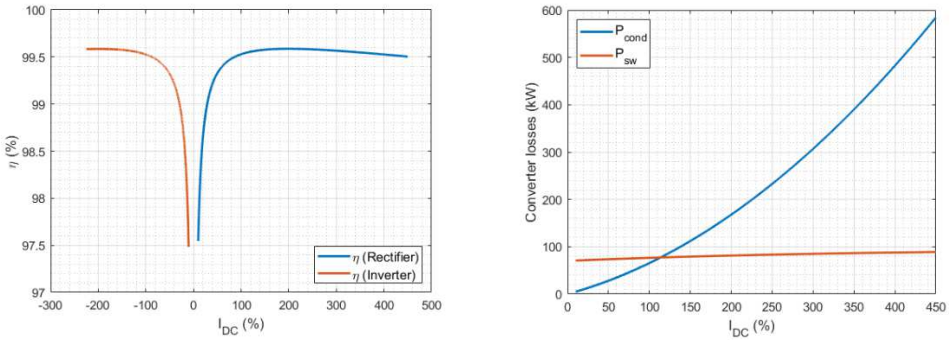

(a) (b)

Fig.3. (a) Power efficiency of 12-pulse thyristor rectifier and inverter (b) Switching and conduction losses of 12-pulse thyristor rectifier

B) Cascaded two-level VSC

Two-level VSC is mainly used in battery energy storages systems, Uninterruptible Power Supplies (UPS), lifts and cranes [18]. ABB group has implemented two-level VSC in a small scale HVDC transmission network, with the voltage of 20 kV DC and the power rating of 3 MW [19], [20]. For the MVDC railways, one of the feasible arrangements is to connect several two-level VSCs in series to form a cascaded topology, as shown in Fig. 4 (a).

The IGBT-Diode module ABB 5SJA 3000L520300 [22] is chosen to implement two-level VSCs. The maximum collector-emitter voltage and maximum DC collector current (I_C) for this module are 5.2 kV and 3 kA, respectively. The switches (switching blocks) in each two-level VSC must block the DC link voltage and carry the current $I_{AC,peak,overload}$ in the worst case. Because of overvoltage at the AC side and existence of stray inductances in the circuit, the applied voltage to the 5.2 kV module should not exceed 2.6 kV ($V_{CES,max}$) [15]. Therefore, to avoid series connection of IGBT-Diode modules in the switching blocks, the DC link voltage for each two-level VSC is chosen to be 2.6 kV.

The cascaded converter must tolerate the maximum voltage of the MVDC system (U_{max3}) at the DC side. Hence, the number of required two-level VSC converters is $N_{two-level} = ceil\left(\frac{U_{max3}}{V_{CES,max}}\right) = 15$.

In each two-level VSC, the peak value of the AC side line-to-line voltage is lower than DC side voltage. Considering voltage drop in the TPS transformer and variation of AC voltage, the ratio between these two voltages at nominal condition is chosen to be 1.2. Based on the method presented in [21], assuming negligible losses, and operating the two-level VSC converters with unity power factor, the nominal phase current at the AC side of each two-level VSC is calculated as follows:

$$\frac{\sqrt{3}}{2} V_{AC,L-L,peak} I_{AC,phase,peak} = V_{DC,nom} I_{DC,nom} \quad (11)$$

$$I_{AC,phase,peak} = 1.51\ kA,\ V_{AC,L-L,peak} = 2.17\ kV,\ I_{AC,phase,peak,overload} = 6.80\ kA \quad (12)$$

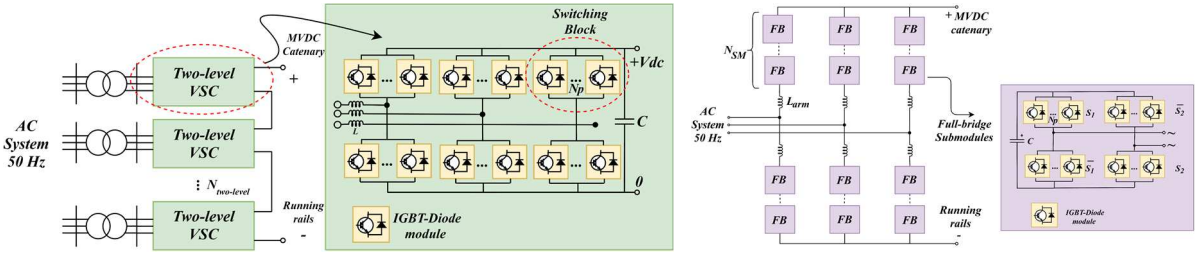

(a) (b)

Fig. 4. (a) Cascaded Two-level VSC (b) MMC-FB and full-bridge submodule

Therefore:

$$N_p = ceil\left(\frac{I_{AC,peak,overload}}{I_C}\right) = 3 \quad (13)$$

where N_p are the number of parallel modules in each switching block of each two-level VSC. Considering the modulation index to be m = 1, the conduction losses of each IGBT-Diode module can be calculated as follows [21]:

$$P_{conduction\ losses,IGBT} = \frac{V_{TH-IGBT}\, I_{AC,peak,module}}{2\pi}\left(1+\frac{\pi}{4}\right) + \frac{r_{IGBT} {I_{AC,peak}}^2}{8}\left(1+\frac{8}{3\pi}\right) \quad (14)$$

$$P_{conduction\ losses,diode} = \frac{V_{TH-Diode}\, I_{AC,peak,module}}{2\pi}(1-0.2\pi) + \frac{r_{Diode} {I_{AC,peak}}^2}{8}\left(1-\frac{6.4}{3\pi}\right) \quad (15)$$

$$P_{conduction\ losses,module} = P_{conduction\ losses,IGBT} + P_{conduction\ losses,diode} \quad (16)$$

where V_{TH} and r are threshold voltage and slope resistance of the IGBT and diode. The switching losses can be determined as follows [21], [23]:

$$P_{switching\ losses,IGBT} = \frac{I_{AC,peak,module}\, f_s}{\pi} \frac{E_{swIGBT}\,(I_{swIGBT})}{I_{swIGBT}} \frac{V_{CES,max}}{V_{cc}} \quad (17)$$

$$P_{switching\ losses,diode} = \frac{I_{AC,peak,module}\, f_s}{\pi} \frac{E_{swDiode}\,(I_{swDiode})}{I_{swDiode}} \frac{V_{CES,max}}{V_{cc}} \quad (18)$$

where f_s is the switching frequency, and E_{swIGBT} is the summation of turn-on and turn-off switching energy of IGBT ($E_{on} + E_{off}$). According to [21] and using linear approximation, the E_{swIGBT} is proportional to the collector current. The parameter $E_{swIGBT}(I_{swIGBT})$ is corresponding switching energy at the current I_{swIGBT}, which is chosen as IGBT rated current. For the diode, $E_{swDiode}$ is turn-off switching energy, and $I_{swDiode}$ is defined similar to I_{swIGBT}. The variable $I_{AC,peak,module}$ is the peak of AC current which flows through each module.

The data provided for switching energy losses in the datasheet is collected at DC link voltage of V_{cc}. However, the actual applied voltage on each IGBT-Diode module is $V_{CES,max}$. Therefore, a correction factor is applied in the last term of (17) and (18). The total losses of the converter are determined as follows:

$$P_{total\ losses,converter} = N_{two-level} \times 6 \times N_p \times \left(P_{conduction\ losses,IGBT} + P_{conduction\ losses,diode} + P_{switching\ losses,IGBT} + P_{switching\ losses,diode}\right) \quad (19)$$

Table III shows losses of the cascaded two-level VSC in nominal DC current, evaluated for different switching frequencies and in rectifier mode of operation. Considering switching frequency of 1 kHz, the efficiency is 1.9% less than the 12-pulse rectifier. Fig. 5 (a) shows the conduction and switching losses of the converter, delivering nominal DC voltage, and operating with switching frequency of 1 kHz. The switching losses is the dominated part of losses and grow faster than conduction losses. In contrast to the 12-pulse rectifier, the switching losses of the cascaded two-level VSC are highly dependent on the DC current. Fig. 5 (b) shows the effect of switching frequency on the power losses. Increasing switching frequency leads to higher switching losses which dramatically degrades the power efficiency. As Fig. 5 (b) suggests, 5 kHz is not a reasonable choice for the switching frequency.

C) MMC-FB

MMCs are used in wide range of voltages and powers, from MVDC to HVDC applications including motor drives, Static Synchronous Compensators (STATCOMs), multi-terminal HVDC systems and collection networks in offshore wind farms [24].

Table III: Cascaded two-level VSC losses in nominal DC conditions

Losses \ f_s(kHz)	1	2	3
$P_{conduction\ losses,module}$ (kW)	0.30	0.30	0.30
$P_{switching\ losses,module}$ (kW)	2.34	4.68	7.02
$P_{total\ losses,converter}$ (kW)	712.71	1,344.84	1,976.97
$\eta_{converter}$ (%)	97.68	95.71	93.81

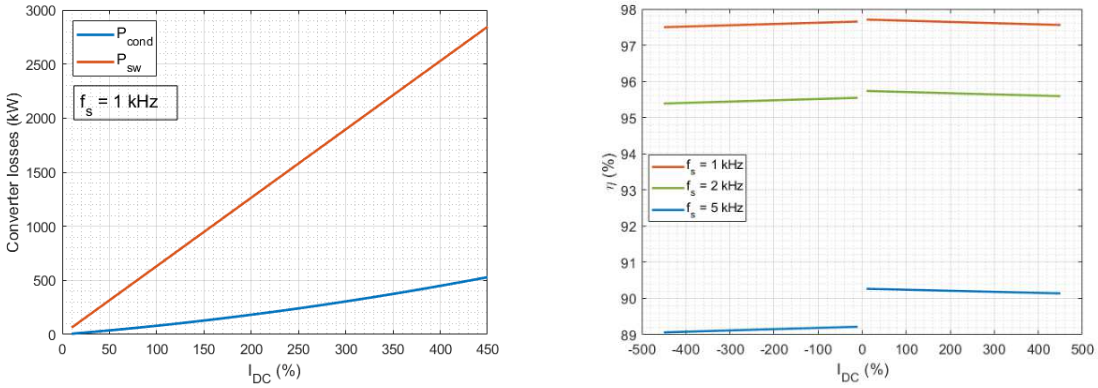

(a) (b)

Fig. 5. (a) Switching and conduction losses of cascaded two-level VSC in switching frequency of 1 kHz (b) Cascaded two-level VSC power efficiency in different switching frequencies

In the full-bridge submodule, there are four switching blocks with N_p parallel IGBT-Diode modules, as shown in Fig. 4 (b). Based on the method presented in [25] and using the same IGBT-Diode module of the previous case (5SJA 3000L520300) [22], an MMC-FB is designed for the MVDC TPS. The converter is designed for U_{max3} and it is desired to avoid series connection in the switching devices. Hence, the number of required submodules in each arm is $N_{SM} = ceil\ (\frac{38.75\ kV}{2.6\ kV})$ = 15 and there are six arms in MMC-FB. The capacitor voltage in each submodule ($V_{C,n}$) is $\frac{27.5\ kV}{15\ kV}$ = 1.83 kV and the capacitance of each submodule is 6.9 mF. The converter is considered to operate with unity power factor and negligible losses. In nominal operating condition:

$$V_{AC,phase,peak} = \frac{1}{2} m\, V_{DC,nom} \tag{20}$$

$$\frac{3}{2} V_{AC,phase,peak,nom} I_{AC,phase,peak,nom} = V_{DC,nom}\, I_{DC,nom} \tag{21}$$

$$V_{AC,phase,peak,nom} = 13.75\ kV,\ \ I_{AC,phase,peak,nom} = 1.45\ kA,$$
$$I_{AC,phase,peak,overload} = 6.55\ kA \tag{22}$$

where m is modulation index which is assumed to be 1 in the calculations. Each switching device must be able to deliver the peak arm current in overload condition:

$$I_{arm}(t) = \frac{I_{DC}}{3} \pm \frac{I_{AC,\mathrm{phase},peak}}{2} \cos(\omega t) \tag{23}$$

$$(I_{arm,peak})_{max} = \frac{I_{DC,overload}}{3} + \frac{I_{AC,phase,peak,overload}}{2} = 4.91\ kA \tag{24}$$

$$N_p = ceil\ (\frac{(I_{arm,peak})_{max}}{I_C}) = 2 \tag{25}$$

To evaluate conduction and switching losses of the submodules, it is necessary to determine the time intervals when semiconductors (diodes and IGBTs) are conducting. This depends on the submodules' operating mode (active or bypassed) and the submodules' current polarity, which are dictated by the control system.

In this paper, the approximate models presented in [26] are used. In the full-bridge submodule, two semiconductors are conducting in every time instant, regardless of the operating mode and current polarity. Thus, the submodule's behaviour is approximated with two semiconductors whose characteristics are a weighted combination of IGBT and diode characteristics:

$$V_{TH-SM} = 0.5\,V_{TH-Diode} + 0.5\,V_{TH-IGBT} \quad (26)$$

$$r_{TH-SM} = 0.5\,r_{Diode} + 0.5\,r_{IGBT} \quad (27)$$

Considering N_p parallel modules in each switching block, conduction losses of each submodule is calculated as follows [26]:

$$I_{arm,rms} = \sqrt{\frac{{I_{AC,\text{phase},peak}}^2}{8} + \frac{{I_{DC}}^2}{9}} \quad (28)$$

$$I_{arm,avgmag} = \frac{1}{2\pi}\int_0^{2\pi}|I_{arm}(t)|\,d\omega t = \frac{1}{\pi}\left(\frac{I_{DC}}{3}(2\theta - \pi) + I_{AC,phase,peak}\,\sin\theta\right);$$

$$\theta = \cos^{-1}\left(\frac{-2\,I_{DC}}{3\,I_{AC,phase,peak}}\right) \quad (29)$$

$$P_{conduction\ losses,SM} = 2\,N_p\left(V_{TH-SM}\frac{I_{arm,avgmag}}{N_p} + r_{TH-SM}\left(\frac{I_{arm,rms}}{N_p}\right)^2\right) \quad (30)$$

where $I_{arm,avgmag}$ is the average current of the equivalent semiconductor, which equals to the average of magnitude of the arm current. As mentioned in section B, the switching energies of IGBT and diodes can be approximated using linear function. In this section, the diode turn-off energy is modelled with a piecewise-linear function:

$$E_{on,IGBT} = k_{on}I_{IGBT}\frac{V_{C,n}}{V_{cc}},\ E_{off,IGBT} = k_{off}I_{IGBT}\frac{V_{C,n}}{V_{cc}} \quad (31)$$

$$E_{sw,diode} = (k_1 + k_2 I_D)\frac{V_{C,n}}{V_{cc}} \quad (32)$$

Assuming switching events to be uniformly distributed over the cycle, the switching losses can be determined using (33):

$$P_{switching\ losses,SM} = N_p f_{sw,m}\frac{V_{C,n}}{V_{cc}}\left(k_1 + \frac{I_{arm,avgmag}}{N_p}\,(k_{on} + k_{off} + k_2)\right) \quad (33)$$

$$P_{total\ losses,SM} = P_{switching\ losses,SM} + P_{conduction\ losses,SM} \quad (34)$$

$$P_{total\ losses,MMC} = 6 \times N_{SM} \times P_{total\ losses,SM} \quad (35)$$

where $f_{sw,m}$ is the switching frequency of the submodule. The loss analysis of the MMC-FB for nominal DC current and in rectifier mode of operation is presented in Table IV.

Fig. 6 (a) shows the power efficiency for different modulation indices. If the current is smaller than $I_{DC,nom}$, the modulation index has limited effect on the power efficiency. The efficiency of MMC-FB is greater than cascaded two-level but lower than the 12-pulse thyristor converter. Fig. 6 (b) represents the switching and conduction losses of the MMC-FB. If the current is higher than 120% of $I_{DC,nom}$, the conduction losses are the dominant part of the losses.

Conclusion

In this paper, thyristor converter, cascaded two-level voltage source converter, and modular multilevel converter with full-bridge submodules are designed and compared for the MVDC TPS. The nominal ratings, number of required semiconductor components, and power efficiency of each topology are analytically evaluated.

The analytical calculations include approximations such as linearisation of conduction characteristics, independence on the temperature, and using maximum or typical values stated in the datasheets. Nevertheless, they provide a useful base for comparing these topologies.

There are also other factors that must be considered in the comparison. For instance, connecting high numbers of series semiconductors requires voltage divider circuits and accurate gate circuits, causing increase in cost and design efforts of the converter. In addition, to make a fair comparison, the topologies must be compared in the same waveform quality at the DC and AC side. According to the analyses presented in this paper and the existing background [21], Table V compares the performance of each topology.

The ability of limiting DC side fault currents is highly desirable in MVDC TPSs, as it enables the protection system to use DC circuit breakers with lower current ratings and costs. Thus, the highly efficient thyristor converters which can control the DC fault currents by thyristors' gate signals are proper candidates for the MVDC TPSs. However, the power factor and harmonic quality reduce substantially when the DC voltage is regulated.

On the other hand, the MVDC railway electrification system is a multi-terminal DC network, whose power flow and voltage profile must be controlled. MMC-FBs are good options for implementing

MVDC networks, thanks to their flexibility in controlling DC side voltage as well as active and reactive power at the AC side with near unity power factor for all loads. The MMC-FBs are also capable of limiting the DC side fault currents and present high quality of the AC currents and do not require the series connection of semiconductor devices. The drawbacks are a lower efficiency than thyristor converters and the need of paralleling IGBTs.

Table IV: Loss analysis of MMC-FB in nominal DC current, $f_{sw,m}$ = 150 Hz and m = 1

$I_{arm,rms}$	0.63 kA	$P_{total\ losses,SM}$	3.68 kW
$I_{arm,avgmag}$	0.52 kA	$P_{total\ losses,MMC}$	331.51 kW
$P_{conduction\ losses,SM}$	1.97 kW	η_{MMC}	98.90 %
$P_{switching\ losses,SM}$	1.71 kW		

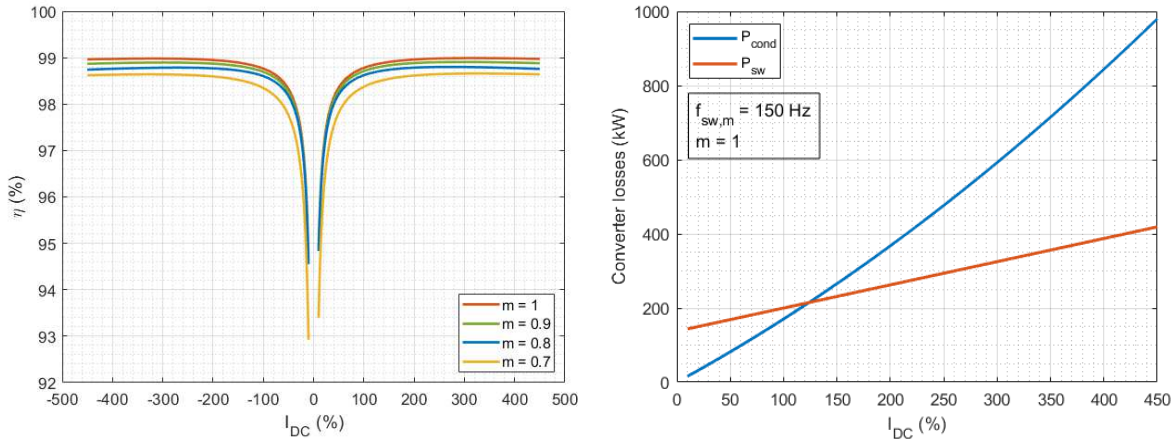

(a) (b)

Fig. 6. (a) MMC-FB Power efficiency in various modulation indices (b) Switching and conduction losses of MMC-FB

Table V: Comparison of topologies

Topology / Factor	Cascaded two-level VSC	Anti-parallel 12-pulse thyristor converters	MMC-FB
Power efficiency	Moderate	High	Moderate
Reactive power performance	Fully controllable	Only consuming	Fully controllable
DC voltage regulation	Excellent	Good	Excellent
Number of semiconductor modules	Moderate	Moderate	High
Need of series semiconductors	Low	High	Low
Transformer (quantity)	Two windings (15)	Three windings (2)	Two windings (1)
Controller complexity	Moderate	Low	High
Harmonic pollution	Low	Moderate	Low
The ability of limiting DC short circuit current	No	Yes	Yes
Possibility of Interference with communication lines	Possible	Unlikely	Possible

References

[1] L. Murray and N. Bottrell, “Riding Sunbeams: Powering our railways with solar PV,” 10:10 Climate

Action, United Kingdom, Tech. Report., 2017. [Online]. Available: https://www.ridingsunbeams.org/reports.

[2] A. Gómez-Expósito, J. M. Mauricio, and J. M. Maza-Ortega, "VSC-based MVDC railway electrification system," *IEEE Trans. Power Deliv.*, vol. 29, no. 1, pp. 422–431, 2014, doi: 10.1109/TPWRD.2013.2268692.

[3] X. He, J. Peng, P. Han, Z. Liu, S. Gao, and P. Wang, "A novel advanced traction power supply system based on modular multilevel converter," *IEEE Access*, vol. 7, pp. 165018–165028, 2019, doi: 10.1109/ACCESS.2019.2949099.

[4] A. Verdicchio, P. Ladoux, H. Caron, and C. Courtois, "New medium-voltage DC railway electrification system," *IEEE Trans. Transp. Electrif.*, vol. 4, no. 2, pp. 591–604, 2018, doi: 10.1109/TTE.2018.2826780.

[5] M. P. Bader and E. V Sachkova, "Adaptation of a traction DC power system for high-speed traffic," *Russ. Electr. Eng.*, vol. 88, no. 9, pp. 573–578, 2017, doi: 10.3103/S1068371217090024.

[6] M. P. Badjor, "Energy effectiveness and electromagnetic compatibility of DC traction power supply systems with 24-kV grid voltage," *Russ. Electr. Eng.*, vol. 82, no. 8, p. 416, 2011, doi: 10.3103/S1068371211080037.

[7] P. Leander and S. Ostlund, "A concept for an HVDC traction system," in *International Conference on Main Line Railway Electrification 1989*, 1989, pp. 169–173.

[8] R. Vial, D. Riu, and N. Retière, "Simulating calculations and optimization design of a new HVDC supply power for light rail system," in *IECON 2010 - 36th Annual Conference on IEEE Industrial Electronics Society*, 2010, pp. 2364–2369, doi: 10.1109/IECON.2010.5675339.

[9] L. Abrahamsson, T. Kjellqvist, and S. Ostlund, "High-voltage DC-feeder solution for electric railways," *IET Power Electron.*, vol. 5, no. 9, pp. 1776–1784, 2012, doi: 10.1049/iet-pel.2011.0219.

[10] *Railway applications - Supply voltages of traction systems*. BS EN 50163:2004 + A1:2007, 2007.

[11] R. D. White, "DC electrification supply system design," in *2007 3rd IET Professional Development Course on Railway Electrification Infrastructure and Systems*, 2007, pp. 35–62.

[12] V. Gelman, "Braking energy recuperation," *IEEE Veh. Technol. Mag.*, vol. 4, no. 3, pp. 82–89, 2009.

[13] E. W. Kimbark, *Direct current transmission*, vol. 1. John Wiley & Sons, 1971.

[14] ABB, "5STP 18M6500 Phase control thyristor," 5STP 18M6500 datasheet, 2013.

[15] ABB, "Voltage ratings of high power semiconductors," 5SYA 2051 application note, 2013.

[16] ABB, "Switching losses for phase control and bi-directionally controlled thyristors," 5SYA 2055-01 application note, 2013.

[17] DYNEX, "Estimation of turn-off losses in a thyristor due to reverse recovery," AN 5951 application note, 2010.

[18] B. Singh, B. N. Singh, A. Chandra, K. Al-Haddad, A. Pandey, and D. P. Kothari, "A review of three-phase improved power quality AC-DC converters," *IEEE Trans. Ind. Electron.*, vol. 51, no. 3, pp. 641–660, 2004, doi: 10.1109/TIE.2004.825341.

[19] G. Asplund, K. Eriksson, and K. Svensson, "DC transmission based on voltage source converters," in *CIGRE SC14 Colloquium, South Africa*, 1997, pp. 1–7.

[20] G. Asplund, "Application of HVDC Light to power system enhancement," in *2000 IEEE Power Engineering Society Winter Meeting. Conference Proceedings (Cat. No. 00CH37077)*, 2000, vol. 4, pp. 2498–2503.

[21] V. Gelman, "Insulated-gate bipolar transistor rectifiers: Why they are not used in traction power substations," *IEEE Veh. Technol. Mag.*, vol. 9, no. 3, pp. 86–93, 2014, doi: 10.1109/MVT.2014.2333762.

[22] ABB, "5SJA 3000L520300 StakPak IGBT Module," 5SYA 1467-01 datasheet, 2018.

[23] ABB, "Applying IGBTs," 5SYA 2053-04 application note, 2013.

[24] S. Du, A. Dekka, B. Wu, and N. Zargari, *Modular multilevel converters: analysis, control, and applications*. John Wiley & Sons, 2017.

[25] K. Sharifabadi, L. Harnefors, H.-P. Nee, S. Norrga, and R. Teodorescu, *Design, control, and application of modular multilevel converters for HVDC transmission systems*. John Wiley & Sons, 2016.

[26] P. S. Jones and C. C. Davidson, "Calculation of power losses for MMC-based VSC HVDC stations," in *2013 15th European Conference on Power Electronics and Applications (EPE)*, 2013, pp. 1–10, doi: 10.1109/EPE.2013.6631955.